Statics and dynamics of incommensurate lattices

G. Theodorou* and T. M. Rice
Bell Laboratories, Murray Hill, New Jersey 07974
(Received 1 February 1978)

We have studied a system of two ionic, interpenetrating, incommensurate sublattices with chain structures. We show that the potential which drives the commensurability between the sublattices varies as $\exp(-2\pi Md/b)$, where b is one lattice period, d is the distance between chains, and the M is the commensurability order. The static distortions in the sublattices, as well as the energy spectrum and the dynamic structure factor of phonons polarized along the chains, are calculated. We conclude that these phonons should be observable in inelastic-neutron-scattering experiments.

I. INTRODUCTION

In recent years, there has been great interest in linear-chain compounds with segregated chains of donors and acceptors. In a number of cases the compounds are not stoichiometric [e.g., $(TTF)(SCN)_{0.545}$ (tetrathiafulvalenium-thiocyanide),[1] $(TTF)I_{0.714}$,[2] $(TTF)Br_{1-x}$,[3] and $Hg_{2.86}AsF_6$ (Ref. 4)] and the periods of the donor and acceptor chains are not simply related. The materials consist of two interpenetrating incommensurate sublattices. In some other cases the two sublattices are commensurate only in high order leading to a large supercell or equivalently a long-wavelength superlattice. In this paper we study the energies of such compounds, especially the energies associated with commensurate states and the dynamics of these states.

As a prototype of these compounds we will consider a model with a two-dimensional array of two types of chains, A and B, with each A chain surrounded by nearest neighbors of type B and vice versa. A two-dimensional analog of our system is shown in Fig. 1. To a lowest approximation we can view each chain as experiencing a rigid external periodic potential due to its neighbors. We call this the external-potential approximation (EPA). The problem of a linear chain of atoms in a periodic external potential has been studied in the context of an adsorbed layer on a substrate. If the chain is replaced by an elastic continuum the problem can be solved exactly and the solution was obtained some years ago by Frank and Van der Merwe.[5] They showed that as the period of the external potential is varied and approaches the natural period of the chain, a continuous transition occurs to the commensurate state in which the period of the chain and the external potential are the same. The discreteness of the chain was considered by Ying,[6] who concluded that the commensurate-incommensurate transitions should be discontinuous or first order. For a discrete chain states with higher-order commensurability are also possible, in which the ratio of the periods of the chain to the external potential is a rational number. Ying[6] obtained first-order results also for transitions between such higher-order commensurate states and the incommensurate state. Recently, Aubry[7] has proven that no first-order transitions occur in this model and that all commensurate-incommensurate transitions are continuous.

Our approach will be to compare the continuum limit to the discrete model and to pass to the continuum limit to describe the actual phase transition between commensurate and incommensurate states. In the incommensurate state the position of the center of mass of the atoms relative to the external potential, described by a phase variable, is undetermined in the ground state, but in a commensurate state this phase is pinned. The pinning

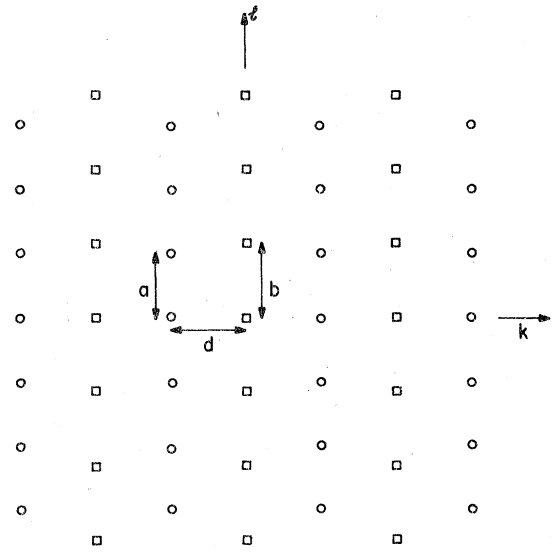

FIG. 1. Two-dimensional analog of a system of two interpenetrating sublattices.

potential, we show, drops off exponentially with the order of commensurability. Similarly it is the pinning potential which enters the effective Frank–Van der Merwe continuum model which describes the transition to a higher-order commensurate state. We also discuss the limit under which the EPA can be expected to be a good approximation.

Small oscillations about the equilibrium positions lead to a phonon spectrum for the lattices. The phonon spectrum is again described by passing to the continuum limit where the problem reduces to one solved analytically by Sutherland.[8] In the external potential approximation each sublattice has an independent acoustical mode in the long-wavelength limit. In commensurate states there is only one acoustical mode and an optical mode with a gap whose magnitude is determined by the pinning potential. Finally we discuss the structure factor and show that these acoustical phonons contribute to the dynamic structure factor and should be observable by inelastic neutron scattering. Actually such independent acoustic modes have been observed at high temperatures for the Hg and AsF_6 sublattices in $Hg_{2.86}AsF_6$ by Hastings *et al.*[9]

In this paper we restrict ourselves to models in which there is a *single* natural period on each chain. The significance of independent natural chain-lattice constants has been emphasized by Phillips[10] in his models of low-temperature lateral phase transitions in compounds which undergo Peierls transition such as TTF-TCNQ (tetrathiafulvalenium-tetracyanoquinodimethanide). These models contain *two* distinct electronic phases on a chain, each with its own natural period. Phillips has also considered the effect of these multiple periodicities on conductivity and other properties.

The paper is organized as follows. In Sec. II we introduce the model and discuss the magnitude of the potential exerted on a chain by its neighbors. In Sec. III we discuss the static arrangement of the atoms in the EPA, especially the relation between the continuum limit and discrete model and the transition to commensurate states. The limitations of the EPA are also considered. The dynamics and phonon spectrum are the subject of Sec. IV. The static and dynamic structure factor is considered in Sec. V. Finally Sec. VI is a summary of our results.

II. POTENTIAL ENERGY

We consider a crystal with a chain structure as described in the Introduction, with two incommensurate sublattices A and B which have periods a and b, respectively. The two sublattices are taken to be oppositely charged and bound together by electrostatic forces. The periods a and b are determined by minimizing the combined intrachain energy, charge-transfer energy, and the Madelung energy due to the long-range Coulomb attraction between chains. This problem has been considered by Torrance and Silverman.[11] In this paper we study the effects of the short-range interaction between chains due to the fact that the two sublattices have different periodicities.

Because of the different periodicities, different sites on the same chain will experience different potentials. More specifically, let us consider one chain of sublattice A. Let $V_a(n)$ be the potential energy at site n, produced by sublattice B. $V_a(n)$ is periodic with period b of sublattice B. Thus, we can expand $V_a(n)$ in harmonics as follows:

$$V_a(n) = \frac{1}{4} \sum_{m=-\infty}^{\infty} U_a(m)\, e^{i(2\pi m/b)na}\,, \tag{2.1}$$

where $U_a(m)$ is given by

$$U_a(m) = \frac{4}{N} \sum_{n=-N/2}^{N/2} e^{-i(2\pi m/b)na} V_a(n)\,, \tag{2.2}$$

with N the number of atoms per chain of sublattice A. Assuming only Coulomb forces

$$V_a(n) = Q_a Q_b \sum_{l,\vec{k}} \frac{1}{|\vec{r}_{n,\vec{0}} - \vec{r}_{l,\vec{k}}|}\,, \tag{2.3}$$

where $r_{l\vec{k}}$ is the position of l ion on a chain whose location is specified by the two-dimensional vector $\vec{k}$ (see Fig. 1). Q_a and Q_b are the charges of ions belonging to sublattices A and B, respectively. For simplicity we consider Q_a and Q_b as point charges. Combining Eqs. (2.1) and (2.3) we obtain

$$U_a(m) = \frac{4Q_aQ_b}{N} \sum_{\vec{k}} \sum_{l} \sum_{n=-N/2}^{N/2} e^{-i(2\pi mna/b)} \frac{1}{[(na - lb - s_{\vec{k}})^2 + d_{\vec{k}}^2]^{1/2}}\,, \tag{2.4}$$

where $s_{\vec{k}}$ is the origin of the $\vec{k}$ chain and $d_{\vec{k}}$ is its distance to the A chain under consideration. $U(0)$ is the Madelung energy and has been incorporated in the determination of a and b as discussed above.

In evaluating $U_a(m)$, for $m \neq 0$, we first sum over n and then over l. Because $[(na - lb - s_{\vec{k}})^2 + d_{\vec{k}}^2]^{-1/2}$ decays slowly, the summation over n can be replaced by integration. In that case Eq. (2.4) reduces to

$$U_a(m) = \frac{4Q_aQ_b}{N} \sum_{\vec{k}} \sum_{l} e^{-i2\pi m(lb + s_{\vec{k}})/b} \times \frac{1}{a} \int_{-Na/2}^{Na/2} dy \, \frac{e^{-i(2\pi m/b)y}}{(y^2 + d_{\vec{k}}^2)^{1/2}} . \quad (2.5)$$

We note that the contributions to $U_a(m)$ from other chains of the sublattice A are identically zero. $U_a(m)$ then becomes

$$U_a(m) = \frac{8Q_aQ_b}{b} \sum_{\vec{k}} K_0\left(\frac{2\pi |m| d_{\vec{k}}}{b}\right) e^{-i2\pi m s_{\vec{k}}/b} , \quad (2.6)$$

with K_0 the zeroth-order Bessel function. Combining Eqs. (2.1) and (2.6) leads to

$$V_a(n) = \frac{4Q_aQ_b}{b} \sum_{m=1}^{\infty} \sum_{\vec{k}} K_0\left(\frac{2\pi m d_{\vec{k}}}{b}\right) \times \cos\left(\frac{2\pi m}{b}(na - s_{\vec{k}})\right) . \quad (2.7)$$

In the present work we restrict ourselves to the case that s is independent of $\vec{k}$. Since K_0 decays exponentially for large values of the argument, only that B chains that are nearest neighbors to the A chain under consideration, will contribute. Also the $m = \pm 1$ harmonics will dominate. Thus,

$$V_a(n) = \tfrac{1}{2} U_a \cos[(2\pi/b)(an - s)], \quad (2.8)$$

with

$$U_a = (8Q_aQ_b/b) z_b K_0(2\pi d/b), \quad (2.8a)$$

where z_b is the number of nearest-neighbor B chains at a distance d from the A chain. For crystals with $d/b \gtrsim 1$, it is appropriate to use the asymptotic behavior of K_0, which gives

$$U_a = 4Q_aQ_b z_b \, (bd)^{-1/2} e^{-2\pi d/b} . \quad (2.9)$$

An order-of-magnitude estimate for the amplitude U_a can be obtained by assuming $b = 3$ Å, $d = 4$ Å, $a/b = 0.8$, $z_b = 4$, and $Q_aQ_b = -e^2a/b$. We then get $U_a = -1.2 \times 10^{-2}$ eV. This estimate would be modified if we consider that the charges are distributed in space and there are not simply point charges.

If instead of focusing on a chain of sublattice A, we examine a chain of sublattice B, calculations similar to those carried out before give

$$U_b = (8Q_aQ_b/a) z_a K_0(2\pi d/a) . \quad (2.10)$$

The asymptotic behavior of U_b is given by

$$U_b = 4Q_aQ_b z_a (ad)^{-1/2} e^{-2\pi d/a} . \quad (2.11)$$

Combining Eqs. (2.8) and (2.11) we obtain the ratio of the first harmonics belonging to chains of A and B sublattices

$$|U_a/U_b| \simeq (a/b)^{1/2} \exp[2\pi d(1/a - 1/b)] . \quad (2.12)$$

The presence of the difference $1/a - 1/b$ in the exponent of (2.12) indicates that the harmonic with the largest amplitude is produced on the chain that has the shortest period. The most signficant feature of U_a and U_b is that they decay exponentially with the distance between nearest-neighbor chains belonging to different sublattices.

We note that the magnitudes of the potentials U_a and U_b are quite small and the corresponding driving forces to commensurability will be weak. This is a consequence of the linear chain structure and the assumption of only Coulomb forces between the chains. This result will be modified if covalent bonding between chains were present and in that case incommensurate structures are not likely to be stable.

III. GROUND STATE

From our calculations of Sec. II we found that each sublattice is under the influence of an external periodic potential created by the other sublattice. Each chain will have a *natural* period along the chain axis; the natural period is defined as the period of the chain in the absence of a spatially varying potential from its neighbors. The natural periods of sublattices A and B are denoted by a and b, respectively. We also assume that a and b are incommensurate and $a < b$.

The presence of the potentials V_i, $i = a, b$ will modify the periods of the sublattices. For $a < b$ we get from (2.12) that $|U_a| > |U_b|$. The latter inequality means that the lattice which will experience the strongest external potential will be sublattice A. For this reason we choose to divide our analysis into two stages: in the first stage, *one sublattice in an external potential*, we assume that sublattice B is rigid with period equal to its natural value b and study the effect on sublattice A of the potential due to B. In the second-stage *two-sublattice problem* both lattices A and B are allowed to distort.

A. One sublattice in an external potential

We begin by studying only *one* chain of sublattice A. The total potential energy of the chain can be written as

$$N\mathcal{E}_a = \tfrac{1}{2}\mu_a \sum_{n=-N/2}^{N/2} (z_{n+1} - z_n - a)^2 + \frac{U_a}{2} \sum_{n=-N/2}^{N/2} \left[1 - \cos\left(\frac{2\pi z_n}{b}\right)\right], \quad (3.1)$$

where z_n denotes the position of the nth atom and we take $U_a > 0$. At zero temperature, the equilibrium positions of the atoms can be found by minimizing $\mathcal{E}_a$. This problem is identical to that

studied by Frank and Van der Merwe[5] for the case of an adsorbed layer on a substrate. The equilibrium position of the nth atom is given by

$$z_{n+1}-2z_n+z_{n-1}=(\pi U_a/\mu_a b)\sin[(2\pi/b)z_n]\,. \tag{3.2}$$

Making the transformation

$$z_n=nb+(b/\pi)\phi_n+\tfrac{1}{2}b\,, \tag{3.3}$$

Eq. (3.2) reduces to

$$\phi_{n+1}-2\phi_n+\phi_{n-1}=-(\pi^2U_a/\mu_a b^2)\sin(2\phi_n)\,. \tag{3.4}$$

Frank and Van der Merwe studied Eq. (3.4) in the continuum limit where $\phi_{n+1}-2\phi_n+\phi_{n-1}$ is replaced by $d^2\phi/dn^2$. The continuum-limit approach is accurate if $\pi^2U_a/\mu_a b^2$ is small. For our case where we have typical values of $U_a\simeq 10^{-2}$ eV, $\mu_a\simeq 10^4$ dyn/cm, and $b\simeq 3$ Å, we obtain $\pi^2U_a/\mu_a b^2\simeq 1.8\times 10^{-2}$. Thus it is justified to go to the continuum limit. Then Eq. (3.4) reduces to

$$\frac{d^2\phi_{(n)}}{dn^2}=-\frac{\pi^2U_a}{\mu_a b^2}\sin(2\phi)\,. \tag{3.5}$$

This is the sine-Gordon equation which can be solved exactly and gives that the equilibrium position z_n of the nth atom is[5]

$$z_n=\begin{cases} nb\,, & \text{for } U_a>U_a^c=\tfrac{1}{8}\pi^2\mu_a(a-b)^2 \\ nb+(b/\pi)\phi_{(n)}+\tfrac{1}{2}b\,, & \text{for } U_a<U_a^c\,. \end{cases} \tag{3.6}$$

$\phi_{(n)}$ can be obtained from

$$\int_0^{\phi}\frac{d\theta}{(1-\beta_a^2\sin^2\theta)^{1/2}}=-n\left(\frac{2\pi^2U_a}{\beta_a^2\mu_a b^2}\right)^{1/2}, \tag{3.7}$$

with β_a an integration constant determined by the minimization of the total energy. β_a is in the range (0, 1) and has the behavior $\lim_{U_a\to 0}\beta_a=0$ and $\lim_{U_a\to U_a^c}\beta_a=1$. The physical picture is that for $U_a>U_a^c$ the lattice is in registry with the external potential. At $U_a=U_a^c$ dislocations appear and the period of the lattice changes continuously approaching a when $U_a\to 0$. Dislocations are separated by a number of atoms R_a given by[5]

$$R_a=\frac{2}{\pi}\beta_a\left(\frac{\mu_a b^2}{2U_a}\right)^{1/2}\int_0^{\pi/2}\frac{d\theta}{(1-\beta_a^2\sin^2\theta)^{1/2}}\,. \tag{3.8a}$$

Near the critical value U_a^c, the number of atoms in a dislocation is given by[5]

$$r_a=\beta_a(\mu_a b^2/2U_a)^{1/2}\,. \tag{3.8b}$$

The potential energy per atom relative to the commensurate state is given by[5]

$$\mathcal{E}_a=\frac{1}{R_a}\{(2\mu_a b^2U_a/\pi^2\beta_a^2)^{1/2}\times[2E(\beta_a)-(1-\beta_a^2)K(\beta_a)]-\mu_a b(b-a)\}\,, \tag{3.9}$$

with $E(\beta_a)$ and $K(\beta_a)$ the complete elliptic integrals of first and second kind, respectively. The asymptotic behavior of β_a near $U_a=0$ and $U_a=U_a^c$ will be useful to our subsequent calculations. Using the asymptotic formulas for $K(\beta_a)$ and $E(\beta_a)$ near $\beta_a=0$ and $\beta_a=1$ and minimizing $\mathcal{E}_a$, when $U_a\simeq U_a^c$, β_a is the solution of

$$1-\beta_a^2=\frac{1-U_a/U_a^c}{\ln[4/(1-\beta_a^2)^{1/2}]}\,, \tag{3.10}$$

while for $U_a\ll U_a^c$, β_a can be derived from

$$\beta_a=\tfrac{1}{2}\pi(U_a/U_a^c)^{1/2}-\tfrac{1}{4}\beta_a^3\,. \tag{3.11}$$

Approximate solutions of Eqs. (3.10) and (3.11) are

$$\beta_a^2\simeq 1+2\frac{1-U_a/U_a^c}{\ln(1-U_a/U_a^c)}\,;\quad \frac{U_a}{U_a^c}\lesssim 1\,,$$
$$\beta_a\simeq\frac{\pi}{2}\left(\frac{U_a}{U_a^c}\right)^{1/2}\,;\quad \frac{U_a}{U_a^c}\ll 1\,. \tag{3.12}$$

For arbitrary values of U_a/U_a^c, β_a can be obtained by numerical minimization of $\mathcal{E}_a$ and the results are plotted in Fig. 2. Also shown are the solutions of Eqs. (3.10) and (3.11).

We analyze $\phi(n)$ in more detail. $\phi(n)$ can be

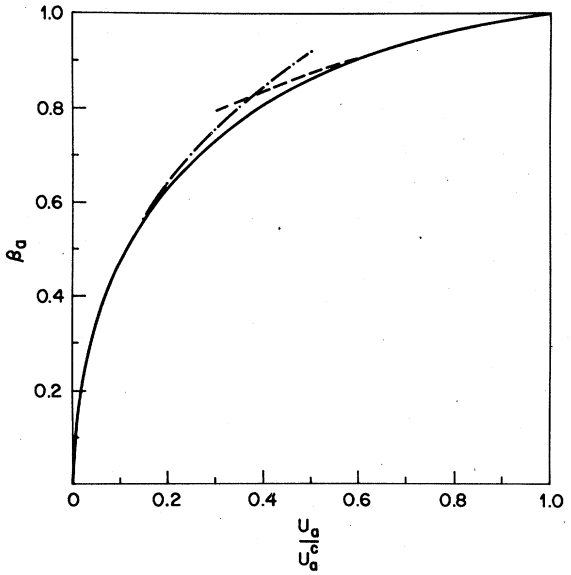

FIG. 2. β_a as a function of U_a/U_a^c. The solid line gives results obtained by numerical minimization of the potential energy [Eq. (3.9)]; the dashed line gives the solution of Eq. (3.10) and the dot-dashed line gives the solution of Eq. (3.11).

written as

$$\phi(n) = am[-n(2\pi^2 U_a/\beta_a^2 \mu_a b^2)^{1/2}] . \quad (3.13)$$

Using the nome expansion of the elliptic integral[12] we obtain that for $U_a < U_a^c$ the position of the nth atom is given by

$$z_n = b\left(1 - \frac{1}{R_a}\right) n - \frac{2b}{\pi} \times \sum_{m=1}^{\infty} \frac{1}{m} \frac{q_a^m}{1+q_a^{2m}} \sin\left(\frac{2\pi m}{R_a} n\right) + \frac{b}{2} , \quad (3.14)$$

where the nome is given by

$$q_a = \exp[-\pi K(\beta_a')/K(\beta_a)] , \quad (3.15)$$

with $\beta_a' = (1-\beta_a^2)^{1/2}$. For n integer Eq. (3.15) becomes

$$z_n = \lambda_a n + \frac{2b}{\pi} \sum_{m=1}^{\infty} \frac{1}{m} \frac{q_a^m}{1+q_a^{2m}} \sin\left(\frac{2\pi m}{b} \lambda_a n\right) \frac{b}{2} , \quad (3.16a)$$

with

$$\lambda_a = b(1 - 1/R_a) . \quad (3.16b)$$

We note that the external potential modifies the position of the atoms. The modified chain is not periodic anymore; instead it has an average period λ_a. The deviations from the average position are described in terms of harmonics whose wave vectors are equal to the reciprocal lattice vectors of the B chain. The amplitude of the harmonics is a function of the expansion parameter q_a, which in turn depends on β_a. Since β_a can be expressed in terms of U_a/U_a^c, we can thus obtain q_a as a function of U_a/U_a^c as shown in Fig. 3. From this figure we see that q_a increases very rapidly near $U_a/U_a^c = 1$. Using the asymptotic formulas for elliptic integrals and Eq. (3.12) we obtain the asymptotic behavior

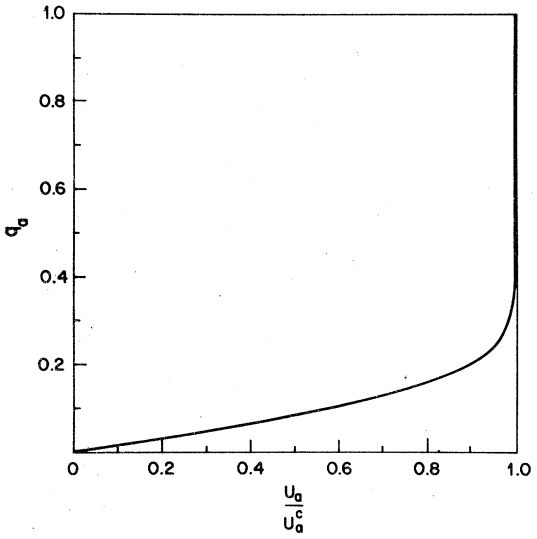

FIG. 3. Nome q_a as a function of U_a/U_a^c.

$$q_a \simeq \begin{cases} \exp\left(-\dfrac{\pi^2}{\ln\{\frac{1}{2}[16U_a^c/(U_a^c-U_a)]\ln[16U_a^c/(U_a^c-U_a)]\}}\right), & \text{for } \dfrac{U_a}{U_a^c} \simeq 1 \\ \dfrac{\pi^2}{64}\dfrac{U_a}{U_a^c}, & \text{for } \dfrac{U_a}{U_a^c} \ll 1 . \end{cases} \quad (3.17)$$

For example, if $U_a/U_a^c = 0.985$, then $q_a = 0.3$. This demonstrates that for all U_a/U_a^c in (0, 1) except for a very narrow range close to 1, q_a is considerably smaller than unity, and therefore only a small number of harmonics in Eq. (3.16) is sufficient to describe z_n. We can understand this physically as follows: a small number of harmonics can describe z_n only if R_a is not considerably larger than r_a. The energy required to produce an extra dislocation for $U_a \simeq U_a^c$ can be obtained from Eq. (3.9) and is given by

$$\epsilon = \mu_a b|b-a|\left[\left(\frac{U_a}{U_a^c}\right)^{1/2} - 1 + 4\left(\frac{U_a}{U_a^c}\right)^{1/2} e^{-\pi R_a/r_a}\right] . \quad (3.18)$$

The equilibrium condition is $\epsilon = 0$. Since the repulsion between dislocations decays exponentially, the ratio R_a/r_a determined by $\epsilon = 0$ in (3.18) is of order of unity except for $U_a/U_a^c \approx 1$. A good estimate of the upper bound of the region where we can use few harmonics to describe z_n is $R_a = 2r_a$, which occurs for $U_a/U_a^c = 0.91$.

Until this point we have used the continuum approximation, but the chain is formed from discrete atoms. It is of interest to compare the discrete and continuum cases. For example, we can expand the position of the atoms in a Fourier series also for the discrete case and obtain[6]

$$z_n = n\lambda_a + \frac{b}{2} + \frac{\pi b}{4} \frac{U_a}{\mu_a b^2} \frac{\sin(2\pi na/b)}{\sin^2(\pi a/b)} + \cdots . \quad (3.19)$$

In the continuum limit a similar expansion is given in (3.14) and this gives

$$z_n = n\lambda_a + \frac{b}{2} + \frac{\pi b}{4} \frac{U_a \sin(2\pi na/b)}{\pi^2 \mu_a (b-a)^2} + \cdots . \quad (3.20)$$

The leading coefficients in the expansion differ only by a numerical factor and in fact in the limit $b \to a$ the expansion coefficients approach each other.

One important difference between the discrete and continuum cases is the possibility of higher-order commensurability in the former case. If $Ma \approx Lb$, where L and M are relative prime integers, then a small U_a will drive the system to a state with average period λ_a such that $M\lambda_a = Lb$. The case $M=1$ is similar to the 1:1 commensurate state and we will not discuss it further. In order to describe the $M:L$ commensurate state for $M>1$, in principle one should keep M harmonics in the atomic position, but a qualitative description of the behavior can be obtained by keeping only the first harmonic. With this restriction the most general form of z_n is

$$z_n = n\lambda_a + \tfrac{1}{2}b + (b/\pi)\,\phi + t\,\sin(2\pi n\lambda_a/b + 2\phi') \,. \tag{3.21}$$

ϕ defines the position of the fundamental period relative to external potential, ϕ' the position of the harmonic relative to the fundamental period, and t is the amplitude of the harmonic. The potential energy per atom for the $M:L$ commensurate state, for $M \geq 3$ is given by

$$\mathcal{E}_a = \tfrac{1}{2}\mu_a(\lambda_a - a)^2 + \mu_a t^2 \sin^2\left(\frac{\pi\lambda_a}{b}\right) + \frac{U_a}{2} - \frac{U_a}{2}\frac{1}{M}\sum_{n=1}^{M}\cos\left(\frac{2\pi}{b}z_n\right). \tag{3.22}$$

The last term on the right-hand side can be simply evaluated for the case of low-order commensurability, e.g., for the 3:1 case is

$$-\frac{U_a}{6}\sum_{n=1}^{\infty}\cos\left(\frac{2\pi}{b}z_n\right) = \frac{U_a}{6}\left\{\cos\left[\frac{2}{3}\pi + 2\phi + \frac{2\pi t}{b}\sin\left(\frac{2}{3}\pi + 2\phi'\right)\right] + \cos\left[\frac{2\pi}{3} - 2\phi + \frac{2\pi t}{b}\sin\left(\frac{2\pi}{3} - 2\phi'\right)\right] + \cos\left(2\phi + \frac{2\pi t}{b}\sin 2\phi'\right)\right\}. \tag{3.23}$$

Ying[6] considered this case also but his answer differs from ours.

For a general order of commensurability the last term on the right-hand side of Eq. (3.22) can be evaluated by expanding in a Bessel function series (for details see Appendix A), leading to

$$-\frac{U_a}{2M}\sum_{n=1}^{M}\cos\left(\frac{2\pi}{b}z_n\right) = -\frac{U_a}{2}J_1\left(\frac{2\pi t}{b}\right)\cos[2(\phi - \phi')] + \frac{U_a}{2}J_{M-1}\left(\frac{2\pi t}{b}\right)\cos[2M\phi' + 2(\phi - \phi')] + O\left(J_{M+1}\left(\frac{2\pi t}{b}\right)\right). \tag{3.24}$$

As indicated previously our interest is mainly in the weak-coupling limit and in this limit the first term on the right-hand side of (3.24) is much larger than the second for $M \geq 3$. Therefore, the difference $\phi - \phi'$ is fixed by this term to be

$$2(\phi - \phi') = 0 \pmod{2\pi} \,. \tag{3.25}$$

Thus there is a strong restoring force keeping primary harmonics to be in phase with the external potential. By contrast, the energy is independent of the value of ϕ for the incommensurate state and for a general commensurate state the restoring force is $\sim t^{M-1}$ for changes in ϕ, with t determined in Appendix A. Thus the potential which pins the phase for the case $M \geq 3$ is $\sim U_a(U_a/\mu_a b^2)^{M-1}$ and in general will be small. This calculation has included only the first harmonic of the potential and the first harmonic of the atomic displacement on the A chain. It is straightforward to see that higher harmonics of the potential which are submultiples of M will also contribute a pinning potential of the same order. In general there will be several contributions to pinning potential all of the same order of magnitude $\sim U_a(U_a/\mu_a b^2)^{M-1}$ or equivalently $\sim \exp(-2\pi Md/b)$. Thus the pinning potential for higher-order commensurate states will be very small.

The case $2:L$, with L odd, is a special one. Here the potential energy per atom is given by

$$\mathcal{E}_a = \tfrac{1}{2}\mu_a(\lambda_a - a)^2 + 2\mu_a t^2 \sin^2 2\phi' + \frac{U_a}{2} - \frac{U_a}{2}\sin(2\phi)\sin\left(\frac{2\pi t}{b}\sin(2\phi')\right) \,. \tag{3.26}$$

Using the variable

$$z = 2t\,\sin(2\phi') \,, \tag{3.27}$$

Eq. (3.26) becomes

$$\mathcal{E}_a = \tfrac{1}{2}\mu_a(\lambda_a - a)^2 + \tfrac{1}{2}\mu_a z^2 + \frac{U_a}{2} - \frac{U_a}{2}\sin(2\phi)\sin\left(\frac{\pi z}{b}\right). \tag{3.28}$$

The ground state of the system is given by (ϕ_0, z_0), where

$$\phi_0 = \tfrac{1}{4}\pi \,, \tag{3.29a}$$

and z_0 is the solution of

$$z_0 = \frac{\pi U_a}{2\mu_a b} \cos\left(\frac{\pi z_0}{b}\right) . \tag{3.29b}$$

Expanding $\mathcal{E}_a$ in terms of the deviation of ϕ and z from their equilibrium positions we obtain

$$\begin{aligned}\mathcal{E}_a = {} & \frac{1}{2}\mu_a(\lambda_a - a)^2 + \frac{1}{2}\mu_a z_0^2 + \frac{U_a}{2}\left[1 - \sin\left(\frac{\pi z_0}{b}\right)\right] \\ & + \frac{1}{2}\left[\mu_a + \frac{\pi^2 U_a}{2b^2}\sin\left(\frac{\pi z_0}{b}\right)\right] \\ & \times (z - z_0)^2 + U_a \sin\left(\frac{\pi z_0}{b}\right)(\phi - \phi_0)^2 . \end{aligned} \tag{3.30}$$

From Eq. (3.30) we see that in the 2:L case it is $\phi - \phi_0$ and $z - z_0$ which are the normal coordinates, with $z - z_0$ a strongly pinned coordinate and $\phi - \phi_0$ a weakly pinned one.

So far we have only considered the commensurate state. Since the pinning potential is weak for a higher-order commensurate state, this suggests we use a continuum model and consider states where $\phi_n \equiv \phi'_n$ but ϕ_n is a slowly varying function of n. The potential energy for $M \geq 3$ then becomes

$$\begin{aligned}\mathcal{E}_a = {} & \frac{1}{N}V^a_{\text{inc}} + \frac{1}{2}\frac{\mu_a}{N}\frac{b^2}{\pi^2}\sum_{n=-N/2}^{n=N/2}(\phi_n - \phi_{n-1})^2 \\ & + \frac{1}{N}\sum_{n=-N/2}^{n=N/2} V_M^{\text{pin}} \cos(2M\phi_n) , \end{aligned} \tag{3.31}$$

where, as we showed above, the pinning potential

$$V_M^{\text{pin}} = \text{const}\, U_a (U_a/\mu_a b^2)^{M-1} . \tag{3.32}$$

If we pass to the continuum limit, this leads at once to a Frank–Van der Merwe[5] problem with a sine-Gordon equation of the form

$$\frac{d^2\phi}{dn^2} = \frac{\pi^2}{2M}\frac{V_M^{\text{pin}}}{\mu_a b^2}\sin(2M\phi) . \tag{3.33}$$

The transition to higher-order commensurate states is similar to the 1:1 transition and the results can be taken over with suitable choice of coupling constants, etc. This approach is consistent with the exact mathematical proof given by Aubry[7] that such higher-order transitions are continuous. This approach will lead to a phase diagram in U_a-b/a space similar to Ying's[6] in outline but with all commensurate-incommensurate transitions continuous.

Another difference between the discrete and continuum cases is the periodic potential known as the Peierls potential[13] which acts on dislocations in a discrete lattice. We have neglected this potential and, at least close to higher-order commensurate transitions, the Peierls potential which varies exponentially in the ratio of dislocation width to the lattice parameter will be very small.

B. Two-sublattice problem

In the two sublattice problem both chains are allowed to distort. With λ_a and λ_b we denote the final average periods of sublattices A and B, respectively. Since the natural period $a<b$, this implies $a \leq \lambda_a \leq \lambda_b \leq b$. The potential energy created by a chain will depend on its average period. In principle it will also depend on the harmonic deviations from the average period. Let us, for instance, examine the harmonic deviations of a chain belonging to sublattice B. The period of these deviations will be λ_a. Therefore the potential produced by them on sublattice A, will have the same period with A and the effect of the harmonic deviations will be to renormalize the mass and the force constant of the A sublattice. In our subsequent calculations we shall ignore these effects of harmonic deviations. The range where such an approximation is valid will be discussed later.

The potential energies of the chains belonging to A and B sublattices, respectively, are given by

$$\begin{aligned} N\mathcal{E}_a = {} & \frac{1}{2}\mu_a \sum_n (z_n - z_{n-1} - a)^2 \\ & + \frac{U_a}{2}\sum_n \left[1 - \cos\left(\frac{2\pi}{\lambda_b} z_n\right)\right] , \\ N'\mathcal{E}_b = {} & \frac{1}{2}\mu_b \sum_n (z'_n - z'_{n-1} - b)^2 \\ & + \frac{U_b}{2}\sum_n \left[1 - \cos\left(\frac{2\pi}{\lambda_a} z'_n\right)\right] . \end{aligned} \tag{3.34}$$

U_a and U_b will depend on the periods λ_b and λ_a, respectively. Their expression is given by (2.8a) and (2.10), with a and b replaced by λ_a and λ_b. The equilibrium positions of the atoms can be obtained in a self-consistent way by minimizing $\mathcal{E}_a$ and $\mathcal{E}_b$. The equations obtained from the minimization are solved in the continuum limit as in the case of the one-sublattice problem. In this latter problem we have studied one chain in an external potential with period larger than the period of the chain. In our present situation, however, the external potential acting on sublattice B has period $\lambda_a < b$. We can treat this case in a similar way and the results are

$$R_b = (2/\pi)\,\beta_b\,(\mu_b \lambda_a^2/2U_b)^{1/2} K(\beta_b) , \tag{3.35a}$$

$$U_b^c = \tfrac{1}{8}\pi^2 \mu_b (\lambda_a - b)^2 , \tag{3.35b}$$

$$\lambda_b = \lambda_a (1 + 1/R_b) , \tag{3.35c}$$

and

$$z_n' = \lambda_b n + \frac{2\lambda_a}{\pi} \sum_{m=1}^{\infty} \frac{1}{m} \frac{q_b^m}{1+q_b^{2m}} \sin\left(\frac{2\pi m}{\lambda_a} \lambda_b n\right) + \frac{\lambda_a}{2} , \tag{3.35d}$$

with $\{z_n'\}$ the equilibrium positions of the atoms of sublattice B, and q_b is defined in a manner similar to Eq. (3.15). The expressions for sublattice A are given in Sec. III A if we replace b by λ_b. Thus

$$\lambda_a = \lambda_b (1 - 1/R_a) . \tag{3.36}$$

The periods λ_a and λ_b are the solutions of the system of Eqs. (3.35c) and (3.36).

Let us now examine the range of validity of our original assumption to ignore the effects of the harmonic deviations from the average periods. For our assumption to be valid, the parameters q_a and q_b must be considerably smaller than unity so that the harmonic deviations be small. As was demonstrated in the one sublattice problem, the requirement q_a, $q_b \ll 1$ is not a severe one and therefore our solution of the two-sublattice problem covers all but a very small section of the incommensurate regime. A situation, however, exists when our analysis is valid even close to the transition. This occurs when the elastic constants of the two sublattices differ substantially. In that case we can consider the sublattice with the largest elastic constant as rigid and the two-sublattice problem reduces to a one-sublattice problem. Also for the case of high-order commensurate states, the driving potentials are small, thus the deviations of atoms from their average positions will be small. Consequently the high-order commensurate states can adequately be described by the EPA.

IV. EXCITATION SPECTRUM

In the present section we study the phonon excitation spectrum of the lattices under consideration. From Eqs. (3.22), (3.24), and (3.25) we obtain that for $M \to \infty$ the energy of the system is independent of the relative phase ϕ of the two sublattices. Consequently, for incommensurate lattices and $U \ll U_c$ so that the positions of the atoms are effectively described by one harmonic only, uniform motion of one sublattice relative to the other along the direction of the chains does not cost any energy. This implies that phonons with polarization along the axis of the chain will differ substantially from the phonons of usual crystals. For polarization perpendicular to the chain we will find the usual branches of optical and acoustical phonons and we shall not consider them.

As we have shown in previous analysis for $q_i \ll 1$, $i = a, b$, we can treat the crystal as consisting of two independent sublattices each under the influence of an external periodic potential created by the other sublattice. We study in detail the phonon spectrum of sublattice A. The potential energy of the A sublattice for motion polarized along the direction of the chains is

$$\begin{aligned} N\mathcal{E}_a = {} & \frac{1}{2}\mu_a \sum_{n,l} (z_{n,l} - z_{n+1,l} - a)^2 \\ & + \frac{1}{2}\mu \sum_{nl} (z_{n,l} - z_{n,l+1})^2 \\ & + \frac{U_a}{2} \sum_{nl} \left[1 - \cos\left(\frac{2\pi}{\lambda_b} z_{nl}\right)\right] . \end{aligned} \tag{4.1}$$

We consider an array of chains all in phase with each other and μ is the shear modulus for displacements of the chains relative to each other. The equation of motion is then given by

$$\begin{aligned} & m_a \frac{d^2 z_{nl}}{dt^2} - \mu_a (z_{n+1,l} - 2z_{n,l} + z_{n-1,l}) \\ & - \mu (z_{n,l+1} - 2z_{n,l} + z_{n,l-1}) = -\frac{\pi U_a}{\lambda_b} \sin\left(\frac{2\pi}{\lambda_b} z_{nl}\right) . \end{aligned} \tag{4.2}$$

Making the transformation

$$z_{n,l} = n\lambda_b + (\lambda b/\pi) f_{n,l} + \tfrac{1}{2}\lambda_b ,$$

Eq. (4.2) transforms to

$$\begin{aligned} & m_a \frac{d^2 f_n}{dt^2} - \mu_a (f_{n+1,l} - 2f_{n,l} + f_{n-1,l}) \\ & - \mu (f_{n,l+1} - 2f_{n,l} + f_{n,l-1}) = \frac{\pi^2 U_a}{\lambda_a^2} \sin(2f_{n,l}) . \end{aligned} \tag{4.3}$$

In the continuum limit Eq. (4.3) becomes

$$m_a \frac{\partial^2 f}{\partial t^2} - \mu_a \frac{\partial^2 f}{\partial n^2} - \mu \frac{\partial^2 f}{\partial l^2} = \frac{\pi^2 U_a}{\lambda_b^2} \sin(2f) . \tag{4.4}$$

It is easy to generalize Eq. (4.4) to the three-dimensional case, in which we have

$$m_a \frac{\partial^2 f}{\partial t^2} - \mu_a \frac{\partial^2 f}{\partial n_3^2} - \mu_1 \frac{\partial^2 f}{\partial n_1^2} - \mu_2 \frac{\partial^2 f}{\partial n_2^2} = \frac{\pi^2 U_a}{\lambda_b^2} \sin(2f) , \tag{4.5}$$

with the z axis parallel to the direction of the chains.

We now consider small oscillations around the static solution, that is,

$$f(\vec{n}, t) = \phi(n_3) + \Psi(\vec{n}, t) ,$$

where ϕ is the solution of Eq. (3.5). Equation (4.5) then reduces to

$$m_a \frac{\partial^2\Psi}{\partial t^2} - \mu_a \frac{\partial^2\Psi}{\partial n_3^2} - \mu_1 \frac{\partial^2\Psi}{\partial n_1^2} - \mu_2 \frac{\partial^2\Psi}{\partial n_2^2} = \frac{2\pi^2 U_a}{\lambda_b^2}\Psi(1-2\sin^2\phi) \ . \quad (4.6)$$

We look for solutions of the form

$$\Psi = \exp[i(k_1 a_1 n_1 + k_2 a_2 n_2 - \omega t)]G(n_3) \ , \quad (4.7)$$

where a_1 and a_2 are the periods along the x and y directions, respectively. Substituting Ψ as given by (4.7) into Eq. (4.6) we obtain

$$\frac{d^2G}{dn_3^2} + \frac{2\pi^2 U_a}{\mu_a \lambda_b^2}\left[\left(1 + \frac{\mu_a\lambda_b^2}{2\pi^2 U_a}\frac{\omega_1^2}{\omega_0^2}\right) - 2\sin^2\phi\right]G = 0 \ , \quad (4.8)$$

with $\omega_1^2 = \omega^2 - (1/m_a)(\mu_1 k_1^2 a_1^2 + \mu_2 k_2^2 a_2^2)$ and $\omega_0 = (\mu_a/m_a)^{1/2}$. Making the transformation

$$z = (2\pi^2 U_a/\mu_a\lambda_b^2\beta_a^2)^{1/2} n_3 \ ,$$

Eq. (4.8) reduces to

$$\frac{d^2G}{dz^2} + \left[\beta_a^2\left(1 + \frac{\mu_a\lambda_b^2}{2\pi^2 U_a}\frac{\omega_1^2}{\omega_0^2}\right) - 2\sin^2\phi\right]G = 0 \ . \quad (4.9)$$

Equation (4.9) has been studied by Sutherland.[8] This equation can be reduced to Lame's equation and is exactly soluble and its eigenfunctions are given by[14]

$$G(z, \alpha_0) = [H(z+\alpha_0)/\Theta(z)]e^{-zZ(\alpha_0)} \ , \quad (4.10)$$

with H, Θ, Z, Jacobian eta, theta, and zeta functions with parameter β_a. ω_1 is determined by

$$1 + \beta_a^2 \ \mathrm{cn}^2(\alpha_0/\beta_a) = \beta_a^2(1 + \omega_1^2/\Omega^2) \ , \quad (4.10a)$$

and the requirement that $Z(\alpha_0)$ be purely imaginary. $\Omega^2 = (2\pi^2 U_a/\mu_a\lambda_b^2)\omega_0^2$ and $\mathrm{cn}(\alpha_0/\beta_a)$ is a Jacobian elliptic function with parameter β_a. The wave vector k_3 along the chain will be determined by[8] $e^{+ik_3\lambda_a n} = e^{-zZ(\alpha_0)}$. Sutherland[8] found that the phonon spectrum consists of two branches. In the lower branch, $\alpha_0 = K + i\gamma$ and the energy is given by

$$1 - \beta_a^2\beta_a'^2 \frac{\mathrm{sn}^2(\gamma/\beta_a')}{\mathrm{dn}^2(\gamma/\beta_a')} = \beta_a^2\left(1 + \frac{\omega_1^2}{\Omega^2}\right) \ , \quad (4.11a)$$

while in the upper branch $\alpha_0 = i\gamma$ and the energy is

$$1 + \frac{\beta_a^2}{\mathrm{cn}^2(\gamma/\beta_a')} = \beta_a^2\left(1 + \frac{\omega_1^2}{\Omega^2}\right) \ . \quad (4.11b)$$

$\mathrm{sn}(\gamma/\beta_a')$ and $\mathrm{dn}(\gamma/\beta_a')$ are the Jacobian elliptic functions with parameter β_a'. The lower branch represents the collective modes of the lattice dislocations and has energies in the range $0 \leq \omega_1^2 \leq (\beta_a'^2/\beta_a^2)\Omega^2$. The upper branch corresponds to renormalized phonons and has energies $\omega_1^2 \geq (1/\beta_a^2)\Omega^2$. The energy gap is $\Delta = [(1-\beta_a')/\beta_a]\Omega$. The energy of the lower edge of the gap is $\omega_1^- = [(1-\beta_a^2)^{1/2}/\beta_a]\Omega$ and of the upper edge $\omega_1^+ = (1/\beta_a)\Omega$. In Fig. 4 we plot ω_1^+ and ω_1^- as a function of U_a/U_a^c in units of Ω_c, the value of Ω at $U_a = U_a^c[\Omega_c = \omega_0(2\pi^2 U_a^c/\mu_a\lambda_b^2)^{1/2}]$.

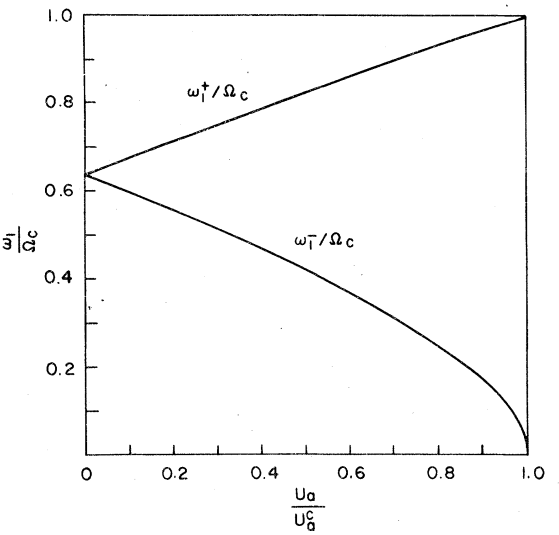

FIG. 4. The energies, ω_1^+ of the upper and ω_1^- of the lower edge of the excitation gap, in units of Ω_c, are plotted as a function of U_a/U_a^c.

We study the long-wavelength limit of the spectrum in detail. The bottom of the lower branch corresponds to $\gamma = K(\beta_a')$. We consider small deviations around this value. For $\gamma = K(\beta_a') - \delta$ we obtain to first order in δ the following relations:

$$iZ[K_a + i(K_a' + \delta)] = \frac{\pi}{2K_a} + \delta\left(1 + \frac{\pi}{2K_aK_a'} - \frac{E_a'}{K_a'}\right) \ ,$$

$$H(z+\alpha_0) \propto e^{-i(\pi/2K_a)z}\,\vartheta_3\left(\frac{\pi z}{2K_a}\right) \times \exp\left[i\delta\frac{d}{dz}\ln\vartheta_3\left(\frac{\pi z}{2K_a}\right)\right] \ ,$$

$$\Theta(z) = \vartheta_4\left(\frac{\pi z}{2K_a}\right) \ , \quad (4.12)$$

where ϑ_3 and ϑ_4 are theta functions; $K_a = K(\beta_a)$, $K_a' = K(\beta_a')$, $E_a = E(\beta_a)$, and $E_a' = E(\beta_a')$. K and E are complete elliptic integrals of first and second kind, respectively. The eigenfunction G will then be given by

$$G(z, K_a + i(K_a' + \delta)) = \frac{\vartheta_3(\pi z/2K_a)}{\vartheta_4(\pi z/2K_a)} \exp\left[i\delta\frac{d}{dz}\ln\vartheta_3\left(\frac{\pi z}{2K_a}\right)\right] \exp\left[i\delta z\left(1 + \frac{\pi}{2K_aK_a'} - \frac{E_a'}{K_a'}\right)\right] . \quad (4.13)$$

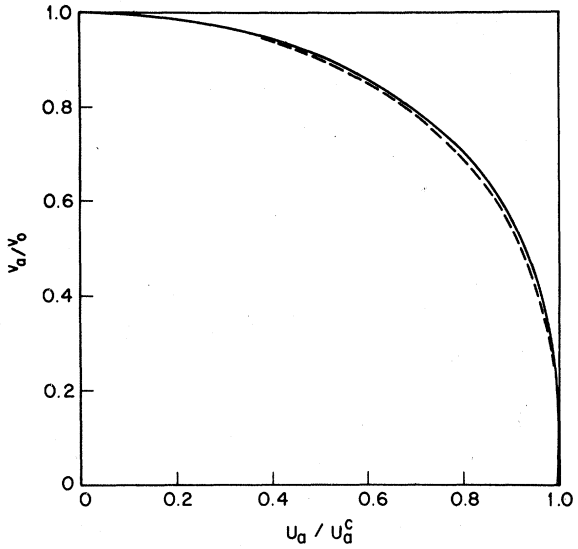

FIG. 5. v_a/v_0 is plotted as a function of U_a/U_a^c, for the case $\lambda_b = b$ and for different values of the ratio a/b. The solid line represents $a/b = 0.8$; the dashed line $a/b = 0.9$.

The wave vector of excitation is

$$k_3 = \frac{\delta}{\lambda_a}\left(\frac{2\pi^2 U_a}{\mu_a \lambda_b^2 \beta_a^2}\right)^{1/2}\left(1+\frac{\pi}{2K_aK_a'}-\frac{E_a'}{K_a'}\right). \tag{4.14a}$$

From Eq. (4.11a) we find that to first order in δ

$$\omega_1 = \beta_1 \delta\omega_0 (2\pi^2 U_a/\mu_a\lambda_b^2\beta_a^2)^{1/2}. \tag{4.14b}$$

Consequently, the sound velocity for propagation along the chains of sublattice A is given by

$$v_a = \frac{d\omega_1}{dk_3} \equiv \frac{\lambda_a \beta_a' \omega_0}{1+\pi/2K_aK_a' - E_a'/K_a'}. \tag{4.15}$$

We note that for β_a approaching zero $\lim_{\beta_a\to 0} v_a = v_0$ $(=a\omega_0)$ is the sound velocity of an independent chain. The sound velocity along the A chains as a function of U_a/U_a^c under the assumption that B lattice is rigid $(\lambda_b = b)$ is shown in Fig. 5. Note v_a depends only weakly on b/a through the factor λ_a. Calculations similar to those outlined above yield a sound velocity

$$v_b = \frac{\lambda_b \beta_b' \omega_0'}{1+\pi/2K_bK_b' - E_b'/K_b'},$$

with $\omega_0' = (\mu_b/m_b)^{1/2}$, for sublattice B. From our analysis it is obvious that for $q_a, q_b \ll 1$ we have two different sound velocities for propagation parallel to the direction of the chains. This analysis assumes infinite chains and ignores the effects of long-range Coulomb interaction and for these reasons is not applicable in the true long-range wavelength limit. This problem requires further study.

The amplitude of oscillation of the nth atom is given by the absolute value of the eigenfunction G at this position. Using the expansion in terms of the nome q_a [see Eq. (3.15)] for the theta functions,[13] we obtain, for long wavelengths

$$|G| = 1 + 4q_a^2 + 4q_a\cos\left(\frac{2\pi\lambda_a}{\lambda_b}n\right) + 4q_a^2\cos\left(\frac{4\pi\lambda_a}{\lambda_b}n\right)+\cdots. \tag{4.16}$$

Thus the amplitude of oscillations of atoms belonging to A chains exhibits periodic variation with period λ_b. Similarly atoms of B chains will oscillate with amplitudes that vary periodically with period λ_a.

Ying,[6] in his study of a submonolayer film adsorbed on a solid surface, has calculated the phonon-dispersion relation via a second-order perturbation expansion. His calculation was done for a discrete lattice under the influence of a rigid periodic external potential with period b. After correcting algebraic errors, we can derive the sound velocity, which in our notation is given by

$$\frac{v_a}{v_0} = \frac{\lambda_a}{a}\left\{1-\left[\left(1-\frac{a}{b}\right)^2\frac{\pi^4 U_a}{16U_a^c}\right]^2\frac{1+\cos^2(\pi\lambda_a/b)}{\sin^4(\pi\lambda_a/b)}\right\}^{1/2}, \tag{4.17}$$

where λ_a in the discrete case, is given, to lowest approximation in U_a by

$$\lambda_a = a - \pi b\left[\left(1-\frac{a}{b}\right)^2\frac{\pi^3 U_a}{32U_a^c}\right]^2\frac{\sin(2\pi a/b)}{\sin^4(\pi a/b)}, \tag{4.18}$$

where $U_a^c = \frac{1}{8}\pi^2\mu_a(a-b)^2$. Results for calculations of λ_a/b and v_a/v_0 for $a/b = 0.9$ are shown in Figs. 6 and 7. For comparison we also include in these figures the results of the continuum model. We

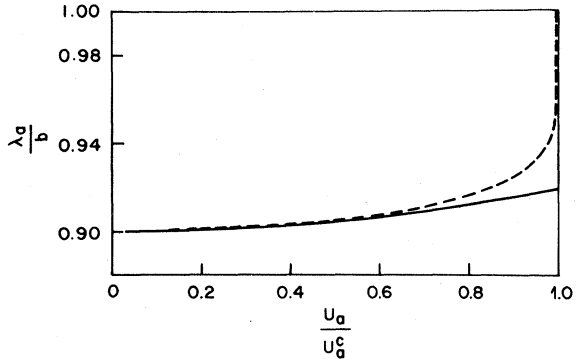

FIG. 6. λ_a/b as a function of U_a/U_a^c. The solid line is the result of perturbation expansion for a discrete lattice [Eq. (4.18)]; the dashed line represents the result of the continuum model [Eq. (3.16b)].

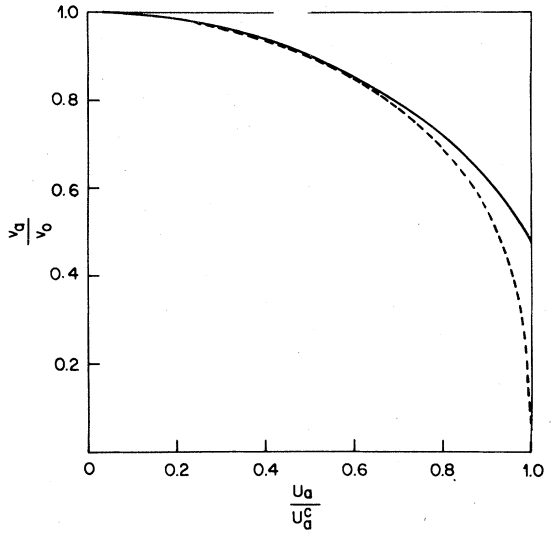

FIG. 7. v_a/v_0 as a function of U_a/U_a^c. The solid line is the result of perturbation expansion for a discrete lattice [Eq. (4.17)]; the dashed line is the result of the continuum model [Eq. (4.15)], for the case $\lambda_b = b$.

note that the exact result in the continuum limit is in good agreement with the second-order perturbation theory in the discrete model except for $U_a \approx U_a^c$. Near the critical potential the renormalization in v_a is large and thus the results of the perturbation expansion are not reliable.

In our study of the excitation spectrum using the continuum approximation, we found that the spectrum has no gap at $k_3 = 0$ when the final periods λ_a and λ_b are incommensurate. In the long-wavelength limit this leads to two different phonon modes on the A and B lattices, respectively. However, as discussed, our analysis neglects long-range Coulomb forces and also the Peierls potential[13] due to the discreteness of the lattice. Both of these approximations require further study in this limit.

We turn now to the case where λ_a and λ_b are commensurate. For 1:1 registry the phonon spectrum has a gap $\Delta = \omega_0 (2\pi^2 U_a/\mu_a \lambda_b^2)^{1/2}$ at $k_3 = 0$. As we discuss in Sec. III, besides the 1:1 commensurability, higher-order commensurate states, e.g., M:L exist. In that case the potential energy of the system is given by Eq. (3.31), and the equilibrium condition is

$$\phi = \pi/2M \ . \tag{4.19}$$

Then considering small oscillations around the equilibrium position, we get that the phonon excitation spectrum of the A sublattice has a gap equal to

$$\Delta_a = (V_M^{\text{pin}}/m_a \lambda_b^2)^{1/2} \ . \tag{4.20}$$

Using Eqs. (2.9) and (3.32) we obtain

$$\Delta_a \propto (\mu_a/m_a)^{1/2} \exp(-\pi d M/\lambda_b) \ . \tag{4.21}$$

Δ_a for the simple cases of 2:1 and 3:1 commensurability is calculated in Appendix B, the results being

$$\Delta_a^{2:1} = (\mu_a/m_a)^{1/2} \, \pi^2 U_a/\mu_a b^2 \ , \tag{4.22a}$$

and

$$\Delta_a^{3:1} = (\mu_a/m_a)^{1/2} (\pi^2 U_a/\mu_a b^2)^{3/2} \ . \tag{4.22b}$$

With regard to the B sublattice, in the general case,

$$\Delta_b \propto (\mu_a/m_b)^{1/2} \exp(-\pi d L/\lambda_a) \ . \tag{4.23}$$

Since $M\lambda_a = L\lambda_b$, Δ_a is of the same order of magnitude with Δ_b. In the actual case of the two interpenetrating sublattices there is only one acoustic mode and an optical mode with an energy gap which decays exponentially with the commensurability order. We note that Lee, Rice, and Anderson[15] in their study of the electron gas with the Fermi vector commensurate to the lattice, proved that the mode involving rigid motion of the CDW against an external periodic potential has an excitation gap $\Delta \propto U_{\text{ext}} (U_{\text{ext}}/t)^{M/2}$, where t is the bandwidth and M the commensurability order, a result similar to ours.

V. STRUCTURE FACTORS

The intensities of x-ray and neutron scattering will be determined by the static and dynamic structure factor. In this section we study the structure factor for each sublattice treating the effect of the other sublattice as a rigid external potential. For this purpose we need to know the equilibrium positions of the atoms, the amplitude of oscillations of the atoms, and the dispersion relation. All these quantities have been calculated previously in the continuum approximation. In our subsequent calculations of the structure factors we assume that the formulas which give the equilibrium positions of the atoms as well as their amplitude of oscillations are those of the continuum model, with the restriction that n, the atom index, be discrete. We also consider that the dispersion relation is that of the continuum model, with a cutoff in the phonon spectrum at the Debye frequency.

The scattering cross section is proportional to the structure factor, the latter being the Fourier transform of $S(\vec{\kappa}, t)$

$$S(\vec{\kappa}, t) = \sum_{\vec{l}\vec{j}} e^{i\vec{\kappa}\cdot(\vec{x}_{\vec{l}} - \vec{x}_{\vec{j}})} \langle e^{-i\vec{\kappa}\cdot\vec{u}_{\vec{l}}(0)} e^{+i\vec{\kappa}\cdot\vec{u}_{\vec{j}}(t)} \rangle \ , \tag{5.1}$$

$\langle \ \rangle$ denotes thermal average, $\vec{\kappa} = \vec{k}_i - \vec{k}_j$ is the momentum transfer, $\{\vec{x}_{\vec{l}}\}$ the equilibrium positions

of the atoms, and $\{\vec{u}_{\vec{l}}(t)\}$ the deviations from equilibrium at time t. We wish to study the effect that phonons with polarization along the direction of the chains will have on the structure factor. Let $\{u_{\vec{l}}(t)\}$ be the displacements along the chain axis. In that case $u_{\vec{l}}(t)$ can be expanded as

$$u_{\vec{l}}(t)=\sum_{\vec{k}}\left(\frac{\hbar}{2m_a\omega(\vec{k})N}\right)^{1/2}\times[\Psi_{\vec{k}}(\vec{l})e^{-i\omega(\vec{k})t}a_{\vec{k}}+\Psi^*_{\vec{k}}(\vec{l})e^{i\omega(\vec{k})t}a^\dagger_{\vec{k}}], \tag{5.2}$$

with $\Psi_{\vec{k}}(\vec{l})=A\exp[i(k_1a_1l_1+k_2a_2l_2)]G_{k_3}(l_3)$, where A is the normalization constant. The parameters a_1 and a_2 have been defined in Sec. IV [Eq. (4.7)].

Combining Eqs. (5.1) and (5.2) leads to

$$S(\vec{\kappa},t)=\sum_{\vec{l}\vec{j}}e^{+i\vec{\kappa}\cdot(\vec{x}_{\vec{l}}-\vec{x}_{\vec{j}})}e^{(\kappa_3^2/2)[u_{\vec{l}}(0),u_{\vec{j}}(t)]}\times\langle e^{-i\kappa_3[u_{\vec{l}}(0)-u_{\vec{j}}(t)]}\rangle\,. \tag{5.3}$$

For small oscillations around the equilibrium position we can consider the motion as harmonic, so that

$$\langle\exp\{-i\kappa_3[u_{\vec{l}}(0)-u_{\vec{j}}(t)]\}\rangle=\exp\{-(\kappa_3^2/2)\langle[u_{\vec{l}}(0)-u_{\vec{j}}(t)]^2\rangle\}. \tag{5.4}$$

The quantities $\langle[u_{\vec{l}}(0)-u_{\vec{j}}(t)]^2\rangle$ and $[u_{\vec{l}}(0),u_{\vec{j}}(t)]$ can be calculated straightforwardly, and the final form of $S(\vec{\kappa},t)$ is given by

$$S(\vec{\kappa},t)=\sum_{\vec{l}\vec{j}}e^{i\vec{\kappa}\cdot(\vec{x}_{\vec{l}}-\vec{x}_{\vec{j}})}\exp\left(-\frac{\hbar\kappa_3^2}{2m_aN}\sum_{\vec{k}}\frac{1}{\omega(\vec{k})}[\psi^*_{\vec{k}}(\vec{l})\psi_{\vec{k}}(\vec{l})+\psi^*_{\vec{k}}(\vec{j})\psi_{\vec{k}}(\vec{j})](2\langle n_{\vec{k}}\rangle+1)\right)\times\left(1+\frac{\hbar\kappa_3^2}{2m_aN}\sum_{\vec{k}}\frac{1}{\omega(\vec{k})}\psi^*_{\vec{k}}(\vec{l})\psi_{\vec{k}}(\vec{j})e^{-i\omega(\vec{k})t}(\langle n_{\vec{k}}\rangle+1)+\frac{\hbar\kappa_3^2}{2m_aN}\sum_{\vec{k}}\frac{1}{\omega(\vec{k})}\psi_{\vec{k}}(\vec{l})\psi^*_{\vec{k}}(\vec{j})e^{i\omega(\vec{k})t}\langle n_{\vec{k}}\rangle\right), \tag{5.5}$$

where $\langle n_{\vec{k}}\rangle$ is the average number of phonons in state $\vec{k}$ and N the number of crystal sites.

A. Debye-Waller factor

The contribution W_1, to the Debye-Waller factor of the main Bragg peaks of the sublattice, from phonons polarized along the direction of the chains is given by the position-independent part of the expression

$$-\frac{\hbar\kappa_3^2}{4m_aN}\sum_{\vec{k}}\frac{1}{\omega(\vec{k})}[\psi^*_{\vec{k}}(\vec{l})\psi_{\vec{k}}(\vec{l})+\psi_{\vec{k}}(\vec{j})\psi_{\vec{k}}(\vec{j})](2\langle n_{\vec{k}}\rangle+1)\,. \tag{5.6}$$

The spatial modulated parts of Eq. (5.6) modify the satellite intensities. In the long-wavelength limit we have

$$\psi^*_{\vec{k}}(\vec{l})\psi_{\vec{k}}(\vec{l})=\frac{1}{1+16q^2}|G(l_3)|^2\simeq\left[1+8q\cos\left(\frac{2\pi\lambda_a}{\lambda_b}l_3\right)+16q^2\cos\left(\frac{4\pi\lambda_a}{\lambda_b}l_3\right)\right]. \tag{5.7}$$

The amplitude of oscillations is independent of $\vec{k}$ in the long-wavelength limit, and we shall assume that this continues to hold for all $\vec{k}$ although some $\vec{k}$ dependence may be present near the gap. Then

$$\frac{\hbar\kappa_3^2}{4m_aN}\sum_{\vec{k}}\frac{1}{\omega(\vec{k})}\psi^*_{\vec{k}}(\vec{l})\psi_{\vec{k}}(\vec{l})(2\langle n_{\vec{k}}\rangle+1)\simeq W_1\left[1+8q\cos\left(\frac{2\pi\lambda_a}{\lambda_b}l_3\right)+16q^2\cos\left(\frac{4\pi\lambda_a}{\lambda_b}l_3\right)\right],$$

where the Debye-Waller factor

$$2W_1=\frac{\hbar\kappa_3^2}{2m_aN}\sum\frac{1}{\omega(\vec{k})}(2\langle n_{\vec{k}}\rangle+1)\,. \tag{5.8}$$

In the long-wavelength limit $\omega(\vec{k})$ can be written as

$$\omega^2(\vec{k})=v_1^2k_1^2+v_2^2k_2^2+v_3^2k_3^2\,, \tag{5.9}$$

where v_i is the sound velocity in the ith direction. Then W_1 can be calculated straightforwardly. For uncorrelated chains $v_1=v_2=0$, leading to $W_1\to\infty$. This implies that uncorrelated chains will have short-range order at finite temperatures. In this particular case our approach needs modification, and we shall not consider it here.

B. Elastic scattering

The structure factor corresponding to elastic scattering is

$$e^{2W_D}S_{\rm el}(\vec{k},t)=\left|\sum_{\vec{l}}e^{i\vec{\kappa}\cdot\vec{x}_{\vec{l}}}\times\exp\left[-8qW_1\cos\left(\frac{2\pi\lambda_a}{\lambda_b}l_3\right)-16q^2W_1\cos\left(\frac{4\pi\lambda_a}{\lambda_b}l_3\right)\right]\right|^2. \tag{5.10}$$

$\vec{x}_{\vec{l}}$ is approximately given by

$$\vec{x}_{\vec{l}} \simeq \vec{x}^{\,0}_{\vec{l}} + \hat{e}_3 \frac{2\lambda_b}{\pi}\left[q \sin\left(\frac{2\pi\lambda_a}{\lambda_b} l_3\right) + \frac{1}{2} q^2 \sin\left(\frac{4\pi\lambda_a}{\lambda_b} l_3\right)\right]. \tag{5.11}$$

with $\{\vec{x}^{\,0}_{\vec{l}}\}$ the positions of the average periodic lattice, and $\hat{e}_3$ the unit vector along the z direction. Using Eq. (5.11) and the generating function for Bessel functions we obtain

$$\sum_{\vec{l}} e^{i\vec{\kappa}\cdot\vec{x}_{\vec{l}}} \exp\left[-8qW_1 \cos\left(\frac{2\pi\lambda_a}{\lambda_b} l_3\right) - 16q^2 W_1 \cos\left(\frac{4\pi\lambda_a}{\lambda_b} l_3\right)\right]$$
$$= N \sum_{\vec{G},\, \alpha_1\alpha_2\alpha_3\alpha_4} J_{\alpha_1}\left(\kappa_3 \frac{2\lambda_b q}{\pi}\right) J_{\alpha_2}\left(\kappa_3 \frac{\lambda_b q^2}{\pi}\right) J_{\alpha_3}(i8qW_1) J_{\alpha_4}(i16q^2 W_1)\, i^{(\alpha_3+\alpha_4)}$$
$$\times \delta\left(\kappa_3 + \frac{2\pi}{\lambda_b}(\alpha_1 - \alpha_3) + \frac{4\pi}{\lambda_b}(\alpha_2 - \alpha_4) - G_3\right) \delta(\kappa_1 - G_1)\, \delta(\kappa_2 - G_2)\,. \tag{5.12}$$

The first-order satellites will appear at $\kappa_3 = G_3 \pm 2\pi/\lambda_b$. We consider the following cases:

(i) $G_3 = 0$. In that case $\kappa_3 = \pm 2\pi/\lambda_b$. The intensity of the satellites relative to an ordinary Bragg reflection is

$$I_{\pm 1}^{G_3=0} \simeq 4q^2(1+2W_1)^2\,. \tag{5.13}$$

We note that both satellites have the same intensity. This is in agreement with the symmetry requirement that the intensities remain invariant under the transformation $\kappa_3 \to -\kappa_3$.

(ii) $G_3 > 0$. Here $\kappa_3 = |G_3| \pm 2\pi/\lambda_b$ and $I_{\pm 1}^{|G_3|}$ is given by

$$I_{\pm 1}^{|G_3|} \simeq q^2[\lambda_b |G_3|/\pi \pm (2+4W_1)]^2\,. \tag{5.14}$$

From Eq. (5.14) we get that the intensity of the two satellites in either sites of G_3 is not the same. This asymmetry comes from two sources: first, the static periodic modulation of the position of the atoms, and second from the fact that atoms oscillate with different amplitudes, the space dependence of the amplitudes being periodic with period that of the external potential. The asymmetry is stronger for large W_1, that is, when $\vec{v}_\perp$ is small. Small values of $\vec{v}_\perp$ mean that we are close to the temperature for which the chains become uncorrelated.

(iii) $G_3 < 0$. In that case $\kappa_3 = -(|G_3| \pm 2\pi/\lambda_b)$ and

$$I_{\pm 1}^{|G_3|} \simeq q^2[\,|G_3|\,(\lambda_b/\pi) \pm (2+4W_1)]^2\,. \tag{5.15}$$

From Eqs. (5.14) and (5.15) we see that satellite spots at $\pm(|G_3| + 2\pi/\lambda_b)$ have the same intensity as required by symmetry. The same is true for the satellites at $\pm(|G_3| - 2\pi/\lambda_b)$.

A general remark for the satellite intensity at $\pm 2\pi/\lambda_b$ is that the latter is proportional to q^2. A similar analysis for satellites at $\pm 4\pi/\lambda_b$ shows their intensity to be proportional to q^4.

C. Inelastic scattering

We will study the inelastic scattering structure factor near the Bragg reflections which correspond to phonon emission, the analysis for the case of phonon absorption being similar. Evaluation of the inelastic structure factor for every $\vec{k}$ is a complicated process and will not be carried out in the present work. Instead we chose to examine the contribution to the structure factor from the region of long wavelengths as well as from the gap edges.

1. Long-wavelength limit

In this limit the contribution to the phonon amplitude G of the term $\exp[i\delta d \ln\vartheta_3(\pi z/2K_a)/dz]$ [see Eq. (4.13)] is unimportant. Also to calculate the structure factor up to second order in q, we need only the first harmonic of G. Thus

$$G = \{1 + 4q^2 + 4q\cos[(2\pi\lambda_a/\lambda_b)\, l_3]\} e^{ik_3 \lambda_a l_3}\,,$$

and the contribution to the structure factor is given by

$$S_{\text{in}}^{L} \simeq \frac{\hbar\kappa_3^2}{2m_a N} \frac{e^{-2W_D}}{1+16q^2} \sum_{\vec{k}} \frac{1}{\omega(\vec{k})} \Bigg| \sum_{\alpha_1\alpha_2} J_{\alpha_1}\left(\frac{q 2\kappa_3 \lambda_b}{\pi}\right) J_{\alpha_2}(i8qW_1)\, i^{\alpha_2}$$
$$\times \sum_{\vec{l}} e^{i(\vec{\kappa}-\vec{k})\cdot\vec{x}^{\,0}_{\vec{l}}} e^{i\alpha_1(2\pi\lambda_a/\lambda_b) l_3} e^{-i\alpha_2(2\pi\lambda_a/\lambda_b) l_3}$$
$$\times [1 + 4q^2 + 2q(e^{i(2\pi\lambda_a/\lambda_b) l_3} + e^{-i(2\pi\lambda_a/\lambda_b) l_3})]\Bigg|^2 e^{-i\omega(\vec{k})t}(\langle n_{\vec{k}}\rangle + 1)\,. \tag{5.16}$$

Since we are interested for the main Bragg reflections only, we have to consider the following four combinations as regards α_1 and α_2: $\alpha_1 = \alpha_2 = 0$; $\alpha_1 = \alpha_2 = \pm 1$; $\alpha_1 = 0$, $\alpha_2 = \pm 1$; $\alpha_2 = 0$, $\alpha_1 = \pm 1$. Then we obtain,

that the contribution to the structure factor from long wavelengths for both one-phonon emission and absorption is given by

$$S_{\rm in}^{L}=e^{-2W_D}NV_c^*\frac{\hbar\kappa_3^2}{2m_aN}\frac{1+2q^2[4-(\kappa_3\lambda_b/\pi)^2+16W_1^2-16W_1]}{1+16q^2}$$
$$\times\sum_{\vec{k}\vec{G}}\frac{1}{\omega(\vec{k})}[\delta(\vec{\kappa}-\vec{k}-\vec{G})e^{-i\omega(\vec{k})t}(\langle n_{\vec{k}}\rangle+1)+\delta(\vec{\kappa}+\vec{k}-\vec{G})e^{i\omega(\vec{k})t}\langle n_{\vec{k}}\rangle], \tag{5.17}$$

where V_c^* is the volume of the reciprocal unit cell. This expression applies only to phonons with long wavelengths along the chain axis. For polarization along the chains we have $\omega(\vec{k}_\perp=0, k_\parallel=(2\pi/\lambda_a)n)=0$. Similarly for the phonon spectrum of the B lattice $\omega(\vec{k}_\perp=0, k_\parallel=(2\pi/\lambda_b)n)=0$. We note that the phonon frequency for the A sublattice vanishes at different points of the reciprocal lattice than the frequency of the B sublattice.

2. Gap edges

The wave vector at the gap is $k_3=\pi/\lambda_a-\pi/\lambda_b$. For such a wave vector the wave function, to first approximation in q, is

$$\psi_{\vec{k}}=\frac{1}{[2(1-2q)]^{1/2}}\left[1+2q\cos\left(\frac{2\pi\lambda_a}{\lambda_b}l_3\right)\right]$$
$$\times(e^{ik_3\lambda_a l_3}\pm e^{-ik_3\lambda_a l_3})e^{i(k_1a_1l_1+k_2a_2l_2)},$$

with the plus (minus) sign corresponding to the lower (upper) edge of the gap. The contribution from $k_3=\pi/\lambda_a-\pi/\lambda_b$ can be calculated in a way similar to that used in the long-wavelength limit. The result is the following:

$$\mathcal{S}_{\rm in}^{G}=e^{-2W_D}NV_c^*\frac{\hbar\kappa_3^2}{4m_aN}\frac{1}{(1\pm2q)}$$
$$\times\sum_{\vec{k}_\perp,\vec{G}}\frac{1}{\omega_\mp(\vec{k})}\delta(\kappa_3\pm k_3-G_3)$$
$$\times[\delta(\vec{\kappa}_\perp-\vec{k}_\perp-\vec{G}_\perp)e^{-i\omega_\mp(\vec{k})t}(\langle n_{\vec{k}}\rangle+1)$$
$$+\delta(\vec{\kappa}_\perp+\vec{k}_\perp-\vec{G}_\perp)e^{i\omega_\mp(\vec{k})t}\langle n_{\vec{k}}\rangle], \tag{5.18}$$

where ω_+ corresponds to upper edge and ω_- to the lower edge of the gap. For $\vec{k}_\perp=0$ we obtain that the structure factor at the gap edges is proportional to

$$\mathcal{S}_-^G(k_\perp=0)\propto\left(\frac{2\pi^2/U_a^c}{\mu_a\lambda_b^2}\right)^{1/2}\frac{1}{1+2q_a}\frac{\omega_0}{\omega_-}$$
$$=\frac{1}{1+2q_a}\left(\frac{\beta_a^2}{1-\beta_a^2}\frac{U_a^c}{U_a}\right)^{1/2}=g_-\left(\frac{U_a}{U_a^c}\right)$$

and

$$\mathcal{S}_+^G(k_\perp=0)\propto\left(\frac{2\pi^2U_a^c}{\mu_a\lambda_b^2}\right)^{1/2}\frac{1}{1-2q_a}\frac{\omega_0}{\omega_+}$$
$$=\frac{1}{1-2q_a}\left(\frac{U_a^c}{U_a}\right)^{1/2}=g_+\left(\frac{U_a}{U_a^c}\right), \tag{5.19}$$

where $\mathcal{S}_-^G$ and g_- correspond to lower edge and $\mathcal{S}_+^G$ and g_+ to upper edge. Formulas (5.19) give a good description of the behavior of the structure factor for $\vec{k}_\perp=0$, provided that $U_a/U_a^c\lesssim0.8$ since in this region $q_a\lesssim0.16$, and therefore higher-order corrections in q_a, which are not included in (5.19), are unimportant. The variation of $g_\pm$ with U_a/U_a^c for $\vec{k}_\perp=0$ and under the assumption that B is rigid ($\lambda_b=b=$ constant) is shown in Fig. 8. From this figure we see that g_+ remains practically unchanged while g_- increases as U_a approaches U_a^c. For $\vec{k}_\perp\neq0$ the variation in $g_\pm$ will become smaller as $\vec{k}_\perp^2$ increases. Our results show that the structure factor at the gap edges are appreciable magnitude and thus the gap in the phonon spectrum should be observable in neutron-scattering experiments.

VI. SUMMARY AND CONCLUSIONS

In this work we studied the static and dynamic behavior of a crystal consisting of two ionic, in-

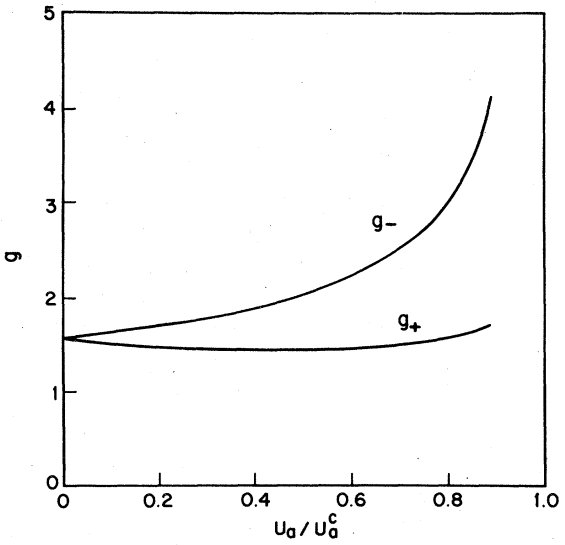

FIG. 8. g^+ and g^-, defined in the text [Eq. (5.22)], as a function of U_a/U_a^c.

terpenetrating sublattices. Each sublattice is under the influence of an external potential created by the other sublattice. Evaluation of the potential showed that it decays exponentially with the distance between nearest-neighbor chains belonging to different sublattices. Also, the sublattice with the biggest period produces the biggest potential.

We treated the problem within the EPA, i.e., we allowed each chain to distort independently due to the presence of an external periodic potential from the other chains. The study of a single chain in an external periodic potential was considered for discrete atoms and also by passing to the elastic-continuum limit. The latter problem is identical to that solved by Frank and Van der Merwe[5] in their study of epitaxial layers. We further analyzed their solution by expanding it in terms of harmonics. The behavior of the expansion as a function of the potential is such, that in the whole region $U < U_{\rm crit}$ we need only a few harmonics to describe the atomic positions z_n, except for a very narrow region close to $U_{\rm crit}$ where a large number of harmonics is needed. A discrete chain of atoms can undergo transition to states of higher-order commensurability and we show that the driving potential decays exponentially with the order of commensurability and that the transition to such states can be approximately described by passing to an appropriate continuum limit which can then be solved exactly.

In the general case where both sublattices are allowed to distort, the rapid convergence of the harmonic expansion enabled us to treat the problem as that of two independent sublattices, each under the influence of an external potential. Then, solving self-consistently we obtained expressions for the final average periods of the sublattices.

We next examined the excitation spectrum of phonons polarized along the direction of the chains. If we consider each chain within the EPA and pass to the continuum limit then the problem reduces to one solved analytically by Sutherland.[8] The solution reveals a linear dispersion at long wavelengths and a gap at a finite wave vector. We calculated the sound velocity along the direction of the chains and found that the sound velocity for propagation along the A chains is different to that along the B chains. The exact result in the continuum limit is in good agreement with second-order perturbation theory in the discrete model except for $U \approx U_{\rm crit}$. In a commensurate state there is only one acoustical mode and an optical mode with energy gap which decays exponentially with the order of commensurability.

Finally we analyzed the structure factor and derived the weight factors of these acoustical phonons in the dynamic structure factor. We concluded that these phonons should be observable in inelastic-neutron-scattering experiments.

The theoretical results derived in this paper are expected to be applicable to materials such as TTF halides and $Hg_{2.86}AsF_6$. A detailed account of these latter applications will be the subject of a separate publication.

APPENDIX A

We are interested to calculate the quantity $\mathcal{E}_a$ defined by Eq. (3.22). Making use of the mathematical identities[16]

$$\cos\left[\frac{2\pi t}{b}\sin\left(\frac{2\pi\lambda_a}{b}n+2\phi'\right)\right] = J_0\left(\frac{2\pi t}{b}\right)+2\sum_{s=1}^{\infty}J_{2s}\left(\frac{2\pi t}{b}\right)\times\cos\left[2s\left(\frac{2\pi\lambda_a}{b}n+2\phi'\right)\right], \quad \text{(A1)}$$

$$\sin\left[\frac{2\pi t}{b}\sin\left(\frac{2\pi\lambda_a}{b}n+2\phi'\right)\right] = 2\sum_{s=0}^{\infty}J_{2s+1}\left(\frac{2\pi t}{b}\right)\sin\left[(2s+1)\left(\frac{2\pi\lambda_a}{b}n+2\phi'\right)\right], \quad \text{(A2)}$$

we obtain

$$-\frac{U_a}{2M}\sum_{n=1}^{M}\cos\left(\frac{2\pi}{b}z_n\right) = -\frac{U_a}{2}J_1\left(\frac{2\pi t}{b}\right)\cos[2(\phi-\phi')]+\frac{U_a}{2}J_{M-1}\left(\frac{2\pi t}{b}\right)\times\cos[2M\phi'+2(\phi-\phi')]+O\left(J_{M+1}\left(\frac{2\pi t}{b}\right)\right), \quad \text{(A3)}$$

where z_n is given by Eq. (3.21). Then the potential energy per atom is given by

$$\mathcal{E}_a = \frac{1}{2}\mu_a(\lambda_a-a)^2+\mu_a t^2\sin^2\left(\frac{\pi\lambda_a}{2}\right)+\frac{U_a}{2} -\frac{U_a}{2}J_1\left(\frac{2\pi t}{b}\right)\cos[2(\phi-\phi')] +\frac{U_a}{2}J_{M-1}\left(\frac{2\pi t}{b}\right)\cos[2M\phi'+2(\phi-\phi')]. \quad \text{(A4)}$$

The ground state is characterized by

$$\phi-\phi' = 0 \pmod{\pi}, \qquad \phi = \pi/2M, \quad \text{(A5)}$$

and by t, which in the weak-coupling limit can be obtained, to $M-1$ order in $U_a/\mu b^2$, from the equation

$$t=\frac{U_a}{4\mu_a \sin^2(\pi\lambda_a/b)}\frac{d}{dt}J_1\left(\frac{2\pi t}{b}\right). \tag{A6}$$

To first order in $U_a/\mu_a b^2$, t is given by

$$t=\frac{\pi U_a}{4\mu_a b \sin^2(\pi\lambda_a/b)}. \tag{A7}$$

APPENDIX B

Consider a chain under the influence of an external periodic potential. Suppose the period a of the undistorted chain, and the period b of the external potential satisfy the relation $Ma=Lb$, with M and L relative prime integers. We calculate the gap in the excitation spectrum of the chain for the special cases: (a) $M=2$, $L=1$ and (b) $M=3$, $L=1$.

A. 2:1 Commensurate state

The configuration of this state is shown in Fig. 9. We define

$$z_2-z_1=\tfrac{1}{2}b-z. \tag{B1}$$

Then

$$z_3-z_2=\tfrac{1}{2}b+z, \tag{B2}$$

and the potential energy of the system is

$$\mathcal{E}_a=\frac{N}{2}\left\{\mu_a z^2+U_a\left[1-\sin\left(\frac{\pi z}{b}\right)\right]\right\}. \tag{B3}$$

The value of z at the equilibrium position is given by the equation

$$z_0=(\pi U_a/2\mu_a b)\cos(\pi z_0/b). \tag{B4}$$

For small displacements from the equilibrium position, the potential energy is

$$\mathcal{E}_a=\frac{N}{2}\left(\mu_a(z+\xi_1-\xi_2)^2+U_a\left\{1-\sin\left[\frac{2\pi}{b}\left(\frac{z_0}{2}+\frac{\xi_1-\xi_2}{2}\right)\right]\times\cos\left[\frac{2\pi}{b}\left(\frac{\xi_1+\xi_2}{2}\right)\right]\right\}\right), \tag{B5}$$

with ξ_1, ξ_2 the displacements of the first and second atom of the supercell, respectively. Then the

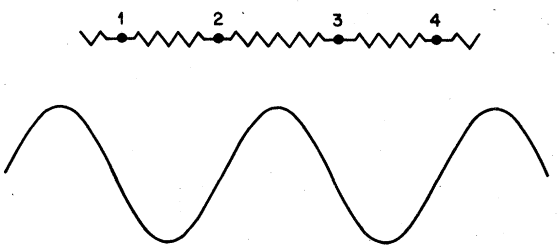

FIG. 9. Configuration of the 2:1 commensurate state.

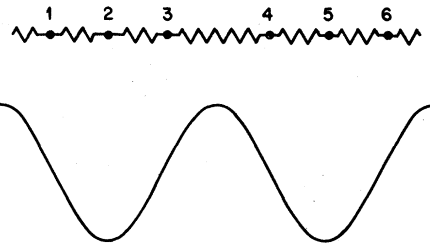

FIG. 10. Configuration of the 3:1 commensurate state.

linearized equations of motion are

$$2m_a\ddot{R}+\frac{4\pi^2U_a}{b^2}\sin\left(\frac{\pi z_0}{b}\right)R=0, \tag{B6a}$$

$$\frac{1}{2}m_a\ddot{r}+\left[2\mu_a+\frac{\pi^2U_a}{b^2}\sin\left(\frac{\pi z_0}{b}\right)\right]r=0, \tag{B6b}$$

with $r=\xi_1-\xi_2$ and $R=\frac{1}{2}(\xi_1+\xi_2)$. The solution of Eq. (B6a) gives that the gap in the lowest branch of the phonon spectrum, to first order in U_a, is given by

$$\Delta_a=(\mu_a/m_a)^{1/2}\pi^2U_a/\mu_a b^2. \tag{B7}$$

We can also obtain the same result starting from Eq. (3.30).

B. 3:1 Commensurate state

The configuration of this state is shown in Fig. 10. We define

$$z_2-z_1=\tfrac{1}{3}b-z \tag{B8}$$

and

$$z_3-z_2=\tfrac{1}{2}b-z. \tag{B9}$$

Thus,

$$z_4-z_3=\tfrac{1}{2}b+2z. \tag{B10}$$

The value of z at the equilibrium position, obtained by minimization of the potential energy, is the solution of

$$z_0=\frac{\pi U_a}{3\mu_a b}\sin\left(\frac{2\pi}{3}-\frac{2\pi z_0}{b}\right). \tag{B11}$$

For small oscillations around the equilibrium position the equations of motion are

$$m_a\ddot{\xi}_1+\left[2+\frac{2\pi^2U_a}{\mu_a b^2}\cos\left(\frac{2\pi}{3}-\frac{2\pi z_0}{b}\right)\right]\xi_1-\xi_2-\xi_3=0, \tag{B12}$$

$$m_a\ddot{\xi}_2-\xi_1+\left(2+\frac{2\pi^2U_a}{\mu_a b^2}\right)\xi_2-\xi_3=0, \tag{B13}$$

$$m_a\ddot{\xi}_3-\xi_1-\xi_2+\left[2+\frac{2\pi^2U_a}{\mu_a b^2}\cos\left(\frac{2\pi}{3}-\frac{2\pi z_0}{b}\right)\right]\xi_3=0, \tag{B14}$$

with ξ_1, ξ_2, ξ_3 the displacements from the equilibrium positions for the first, second, and third atom of the supercell, respectively. From the equation of motion we obtain that the gap in the lowest branch of the spectrum, to first order in U_a, is given by

$$\Delta = (\mu_a/m_a)^{1/2} (\pi^2 U_a/\mu_a b^2)^{3/2} . \quad \text{(B15)}$$

---

*Present address: Department of Physics, University of Crete, Iraklion, Crete, Greece.

[1]F. Wudl, D. E. Schafer, W. M. Walsh, Jr., L. W. Rupp, F. J. DiSalvo, J. V. Waszczak, M. L. Kaplan, and G. A. Thomas, J. Chem. Phys. 66, 377 (1977).
[2]J. J. Daly and F. Sauz, Acta Crystallogr. B 31, 620 (1975).
[3]S. J. LaPlaca, P. W. R. Corfield, R. Thomas, and B. A. Scott, Solid State Commun. 17, 635 (1975).
[4]B. D. Cutforth, Ph.D. thesis (McMaster University, Hamilton, Ontario, 1975); B. D. Cutforth, W. R. Datars, R. J. Gillespie, and A. van Schyndel, Adv. Chem. 150, 56 (1976).
[5]F. C. Frank and J. H. Van der Merwe, Proc. R. Soc. Lond. 198, 205 (1949).
[6]S. C. Ying, Phys. Rev. B 3, 4160 (1971).
[7]S. Aubry (unpublished).
[8]B. Sutherland, Phys. Rev. A 8, 2514 (1973).
[9]J. M. Hastings, J. P. Pouget, G. Shirane, A. J. Heeger, N. D. Miro, and A. G. MacDiarmid, Phys. Rev. Lett. 39, 1484 (1977).
[10]J. C. Phillips, Proc. Natl. Acad. Sci. (U.S.A.) 73, 3820 (1976).
[11]J. B. Torrance and B. D. Silverman, Phys. Rev. B 15, 788 (1977).
[12]M. Abramowitz and I. A. Stegun, *Handbook of Mathematical Functions* (Dover, New York, 1965), p. 591, formula 17.3.24.
[13]J. P. Hirth and J. Lothe, *Theory of Dislocations* (McGraw-Hill, New York, 1968), Chap. 8.
[14]E. T. Whittacker and G. N. Watson, *A Course of Modern Analysis* (Cambridge, U.P., London, 1963). In particular, see Chaps. 20 and 23.
[15]P. A. Lee, T. M. Rice, and P. W. Anderson, Solid State Commun. 14, 703 (1974).
[16]M. Abramowitz and I. A. Stegun, *Handbook of Mathematical Functions* (Dover, New York, 1965), p. 361, formulas 9.1.42 and 9.1.43.